Study on sensitivity analysis method of slope stability based on Sweden arc method

Jing Yu Zhang[1], Liang Peng Wan[2] and Guo Yong Duan[3]

[1]College of Hydraulic and Environmental Engineering, China Three Gorges University, Yichang 443003, China
[2]Wudongde Engineering Construction Department of China Three Gorges Construction Management Co, Ltd, Chengdu 610000, China
[3]College of Civil and Transportation Engineering, Hohai University, Nanjing 210029, China

In this study, an attempt has been made to analyse the impact of different parameters (such as bulk density, cohesive force, internal angle of friction, angle of slip surface and pore water pressure) on the safety factor of a given slope. The analysis was done using the Swedish Arc method. Meanwhile, the sensitivity ratios between different parameters were determined by taking the partial derivatives of non-dimensional parameters. A typical case study with a uniform slope was considered to verify the efficiency of the provided method. The results showed that the change in failure path had a significant impact on the sensitivity ratio of parameters. In the meantime, unstable slopes will have higher value of sensitivity ratio in the shear strength parameters (tan φ and c). The sensitivity analysis method introduced in this article eliminated the crude assumptions made on the conventional approach. The advantage of this analytical method is that both the safety factor and the sensitivity ratio can be computed simultaneously, for slopes with any given slip surface. It is believed that the results will have an indispensable role in understanding and capturing the nature of geotechnical problems.

Keywords: Non-dimensional, partial derivative, sensitivity ratio, sensitivity analysis.

SENSITIVITY analysis has wide applications in many disciplines. In the past, several researchers illustrated the significance of this method. Recently, many practical problems have been solved using sensitivity analysis[1–7].

Sensitivity analysis is a versatile tool. Bonstrom and Corotis[8] used this method for the first-order reliability analysis. Then Ma *et al.*[4] extended the application of this method using advanced integral equation model. Further, a parameterized sensitivity-based finite element model was developed by Park *et al.*[9]. Similarly, sensitivity analysis was employed by using a built-in MATLAB toolbox and ANOVA decomposition conditional Gaussian processes respectively[10,11]. This method was then applied for the advanced energy and multiple response-surface methods respectively[6,12].

Slope stability evaluation using factors' sensitivity analysis plays a vital role in many geotechnical problems, including the most complex hydro powers and cutting slopes. Initially, there were two types of sensitivity analysis used in slope stability evaluation: the first method was single factor sensitivity analysis[13]; and the second was multi-factor orthogonal sensitivity analysis[14]. Later, some modifications were made, and the probability of statistics was introduced into slope reliability analysis to cope up with discreteness, variability and correlations between different factors. No matter which method is used, one should determine the safety factor of a given slope based on certain assumptions. Single-factor sensitivity analysis uses the change in ratio of the safety factor calculated under the following circumstances: a single parameter is varied in a certain range by keeping other parameters constant, and the sensitivity of the parameters is studied. While orthogonal sensitivity analysis uses a change in ratio of the safety factor calculated under the presence of various factors in many groups at different levels, consequently a sensitivity factor is established in a proper order. Though the analysis considers correlations between parameters, it has some drawbacks in the initial design. A reliability sensitivity analysis assumes the incidence factor to meet a certain form of probability distribution, and it considers some variations and correlations among the parameters. However, reliability sensitivity analysis cannot be performed easily for a certain response surface using a multi-factor analysis. In the case of conventional sensitivity analysis, the sensitivity analysis is executed only for shear strength parameters. Meanwhile, it has some limitations in scrutinizing the real engineering problems.

In this study, an attempt has been made to analyse the impact of different parameters (such as bulk density, cohesive force, internal angle of friction, angle of slip surface and pore water pressure) on the safety factor of a given slope. The efficiency of the method was verified using a case study, and a new method of sensitivity analysis for the evaluation of slopes was developed. The new approach proposed in this article can be effectively applied to soil slopes and soil-rock slopes.

Theoretical basis

Many slope stability evaluation tools were developed based on the limit equilibrium approach. This theory

*For correspondence. (e-mail: 364528061@qq.com)

assumes that shear failure along a slip surface will occur when the slope reaches a limit equilibrium state. Therefore, every point on a sliding surface attains a limit equilibrium state, and is defined according to the Mohr-Coulomb failure criterion. In this study, the modified Sweden arc method by Fellenius has been used to study the effects of different parameters on the given slope. Initially, Sweden arc method, developed by Swedish Peterson in 1916, simplifies any slope instability problems into a plane strain condition, and considers an arc shape failure surface. Factor of safety can be determined using the force polygon of the vertical slices as shown in eqs (1)–(3). Both the slide force, S and the skid resistance force, T are expressed as follows

$$S=\sum(W_i \sin\alpha_i),$$

$$T=\sum[c_i' b_i \sec\alpha_i+(W_i\cos\alpha_i-u_i b_i \sec\alpha_i)\tan\varphi_i'], \quad (1)$$

$$S_i=W_i\sin\alpha_i,$$

$$T_i=c_i' b_i \sec\alpha_i+(W_i\cos\alpha_i-u_i b_i \sec\alpha_i)\tan\varphi_i', \quad (2)$$

where i is the slice number, W the weight of the slice, u the pore water pressure acting at the base of the slice, b the width of the slice, α the slope angle along the slip surface, and c' and $\tan\varphi'$ are effective shear strength parameters. For a homogeneous slope, the following assumptions can be made: $c' = c$ and $\tan\varphi' = \tan\varphi$.

Therefore, the safety factor for a particular slip surface is determined by the following equation.

$$F_s=\frac{TR}{SR}=\frac{T}{S}$$

$$=\frac{\sum[c_i' b_i \sec\alpha_i+(W_i\cos\alpha_i-u_i b_i \sec\alpha_i)\tan\varphi_i']}{\sum(W_i\sin\alpha_i)}. \quad (3)$$

It is understood that skid resistance force is mainly affected by shear strength parameters, weight of soil, pore water pressure, and slip surface slope angle. Besides, the slide force is mainly due to the weight of the soil and slope angles on slip surface.

Theoretical derivation

Slope sensitivity analysis studies the correlation between different parameters and the corresponding safety factors. In the conventional method, it is a ratio of change in the safety factor to the change in different parameters. The present study employed the conventional Sweden arc method to investigate the effects of different parameters on the safety factor of a given slope.

Equation (3) can be rewritten in the form of partial derivatives as follows

$$\frac{\partial Fs}{\partial x}=\frac{\frac{\partial T}{\partial x}\cdot S-\frac{\partial S}{\partial x}\cdot T}{S^2}, \quad (4)$$

where x stands for different parameters including: the weight of the slice, W; the pore water pressure acting at the base of the slice, u; the angle of a slip surface, α; and the effective shear strength parameters (c' and $\tan\varphi'$).

As seen from eq. (4), the safety factor will increase when the partial derivative of T increases and S decreases. There are many factors which can manipulate the values of both T and S. Those governing factors are clearly shown in eqs (5) and (6).

$$\frac{\partial S}{\partial W}=\sum\sin\alpha_i, \quad (5)$$

$$\frac{\partial S}{\partial \alpha}=\sum(W_i\cos\alpha_i). \quad (6)$$

The slide force, S increases by an amount of $\sum\sin\alpha_i$ when the weight of slice, W_i increases and the angle of slope remains constant (eq. (5)). Similarly, the slide force, S increases by an amount $\sum W_i\cos\alpha_i$ when the angle of the slope, α_i increases and the weight of the slice remains constant.

The sensitivity of each parameter on the slide force can be computed by the following equations

$$D_W^S=\frac{\partial S}{\partial W}\cdot\frac{W}{S}=\sum\sin\alpha_i\cdot\sum\frac{W_i}{S_i}, \quad (7)$$

$$D_\alpha^S=\frac{\partial S}{\partial \alpha}\cdot\frac{\alpha}{S}=\sum W_i\cos\alpha_i\cdot\sum\frac{\alpha_i}{S_i}, \quad (8)$$

where D_W^S represents the sensitivity of W on S, and D_α^S represents the sensitivity of α on S.

After dividing eq. (7) by eq. (8), the following sensitivity ratio was determined

$$\frac{D_W^S}{D_\alpha^S}=\frac{\sum\sin\alpha_i\cdot\sum\frac{W_i}{S_i}}{\sum W_i\cos\alpha_i\cdot\sum\frac{\alpha_i}{S_i}}. \quad (9)$$

Furthermore, eq. (9) can be rewritten in a more simplified form as shown below

$$\frac{D_{W_i}^{S_i}}{D_{\alpha_i}^{S_i}}=\frac{\sin\alpha_i}{\cos\alpha_i\cdot\alpha_i}=\frac{\tan\alpha_i}{\alpha_i}. \quad (10)$$

The sensitivity ratio of the slide force in a given slope remains constant for a certain ranges of α_i, soil density and angle of a slip surface. For $\alpha_i = \pi/4$ the slide force becomes more sensitive to density than the angle of a slip surface. The skid resistance force has more governing parameters than the slide force. For the purpose of computations, one can use the form of partial derivatives as shown in the following equations

$$\frac{\partial T}{\partial W} = \sum(\cos\alpha_i \cdot \tan\varphi_i'), \quad (11)$$

$$\frac{\partial T}{\partial \alpha} = \sum[c_i' b_i \sec\alpha_i \tan\alpha_i - (W_i \sin\alpha_i + u_i b_i \sec\alpha_i \tan\alpha_i)\tan\varphi_i'], \quad (12)$$

$$\frac{\partial T}{\partial \tan\varphi} = \sum(W_i \cos\alpha_i - u_i b_i \sec\alpha_i), \quad (13)$$

$$\frac{\partial T}{\partial c} = \sum b_i \sec\alpha_i, \quad (14)$$

$$\frac{\partial T}{\partial u} = -\sum(b_i \sec\alpha_i \tan\varphi_i'). \quad (15)$$

The skid resistance force has many governing parameters (eq. (11)). When the internal angle of friction is high the resulting angle of slip surface is small. The skid resistance force is primarily enhanced by the weight of the slice. Equation (12) indicates that the effect of the angle of a slip surface over the skid resistance force is a function of many parameters. The higher values in shear strength parameters and the lower values in weight of the slice and the pore water pressure result in an effective means of the skid resistance force.

The analysis on eq. (13) implies that the skid resistance force that is developed by the internal angle of friction is a function of the weight of the slice, the pore water pressure, and the angle of the slip surface. From eq. (14) it is realized that a significant amount of skid resistance force is developed by cohesion when there is a high angle of slip surface. However, the pore water pressure has an adverse effect on the stability of the slope. The slope has more susceptibility to instability when the angle of the slip surface increases (eq. (15)). In practice, the generation of excess pore water pressure is controlled by means of adequate drainage facilities. Correspondingly, the sensitivity equations are

$$D_W^T = \frac{\partial T}{\partial W}\cdot\frac{W}{T} = \sum(\cos\alpha_i \cdot \tan\varphi_i')\cdot\sum\frac{W_i}{T_i}, \quad (16)$$

$$D_\alpha^T = \frac{\partial T}{\partial \alpha}\cdot\frac{\alpha}{T} = \sum[c_i' b_i \sec\alpha_i \tan\alpha_i - (W_i \sin\alpha_i + u_i b_i \sec\alpha_i \tan\alpha_i)\tan\varphi_i']\cdot\sum\frac{\alpha_i}{T_i}, \quad (17)$$

$$D_{\tan\varphi}^T = \frac{\partial T}{\partial \tan\varphi}\cdot\frac{\tan\varphi}{T} = \sum(W_i \cos\alpha_i - u_i b_i \sec\alpha_i)\cdot\sum\frac{\tan\varphi_i'}{T_i}, \quad (18)$$

$$D_c^T = \frac{\partial T}{\partial c}\cdot\frac{c}{T} = \sum(b_i \sec\alpha_i)\cdot\sum\frac{c_i'}{T_i}, \quad (19)$$

$$D_u^T = \frac{\partial T}{\partial u}\cdot\frac{u}{T} = -\sum(b_i \sec\alpha_i \tan\varphi_i')\cdot\sum\frac{u_i}{T_i}. \quad (20)$$

Usually, major emphasis is given for the sensitivity of shear strength parameters. Hence, the sensitivity of shear strength parameters over skid resistance force is given by eq. (21)

$$\frac{D_{\tan\varphi}^T}{D_c^T} = \frac{\sum(W_i \cos\alpha_i - u_i b_i \sec\alpha_i)\cdot\sum\frac{\tan\varphi_i'}{T_i}}{\sum b_i \sec\alpha_i \cdot \sum\frac{c_i'}{T_i}}. \quad (21)$$

The sensitivity of the shear strength parameters upon the skid resistance force at any given slice is determined as follows

$$\frac{D_{\tan\varphi_i}^{T_i}}{D_{c_i}^{T_i}} = \frac{(W_i \cos\alpha_i - u_i b_i \sec\alpha_i)\cdot\frac{\tan\varphi_i'}{T_i}}{b_i \sec\alpha_i \cdot \frac{c_i'}{T_i}} = \frac{W_i \cos^2\alpha_i \tan\varphi_i'}{b_i c_i'} - \frac{u_i \tan\varphi_i'}{c_i'}. \quad (22)$$

Further analysis is made by using eq. (22): when

$$\frac{W_i \cos^2\alpha_i}{b_i} - u_i > \frac{c_i'}{\tan\varphi_i'} > 0,$$

satisfying the condition

$$W_i \cos\alpha_i > b_i u_i \sec\alpha_i \text{ or } \cos\alpha_i > \sqrt{\frac{b_i u_i}{W_i}}. \quad (23)$$

Equation (23) specifies that the skid resistance force developed by the weight of the slice is much greater than the slide force boosted by the pore water pressure or the angle of the slipping surface. The sensitivity of the internal angle of friction over the skid resistance force, T is much greater than the sensitivity of cohesion.

The sensitivity of different parameters on the safety factor of a given slope is determined by using eq. (4).

$$D_x^{Fs} = \frac{\partial Fs}{\partial x}\cdot\frac{x}{Fs} = \frac{(\partial T/\partial x)\cdot S - (\partial S/\partial x)\cdot T}{S^2}\cdot\frac{x}{Fs}$$
$$= \frac{(\partial T/\partial x)\cdot S - (\partial S/\partial x)\cdot T}{S^2}\cdot\frac{xS}{T}$$
$$= \frac{\partial T}{\partial x}\cdot\frac{x}{T} - \frac{\partial S}{\partial x}\cdot\frac{x}{S} = D_x^T - D_x^S. \quad (24)$$

After merging eqs (7), (8), (16)–(20) and (24), the sensitivity of different parameters over the safety factor of a given slope was determined. For instance, the sensitivity of the shear strength parameters is given below

$$\frac{D_{\tan\varphi}^{Fs}}{D_c^{Fs}} = \frac{D_{\tan\varphi}^T - D_{\tan\varphi}^S}{D_c^T - D_c^S} = \frac{\sum (W_i \cos\alpha_i - u_i b_i \sec\alpha_i)\cdot \sum \frac{\tan\varphi_i'}{T_i}}{\sum b_i \sec\alpha_i \cdot \sum \frac{c_i'}{T_i}}. \quad (25)$$

Further comparisons between the two parameters were done to study the order of importance of each parameter over the safety factor. Mathematically

$$\frac{D_W^{Fs}}{D_\alpha^{Fs}} = \frac{D_W^T - D_W^S}{D_\alpha^T - D_\alpha^S} = \frac{\sum \cos\alpha_i \cdot \tan\varphi_i \cdot \sum (W_i/T_i) - \sum \sin\alpha_i \cdot \sum (W_i/S_i)}{\sum \left[\begin{array}{l} [c_i' b_i \sec\alpha_i \tan\alpha_i - \\ (W_i \sin\alpha_i + u_i b_i \sec\alpha_i \tan\alpha_i)\tan\varphi_i'] \\ \cdot\sum(\alpha_i/T_i) - \sum W_i \cos\alpha_i \cdot \sum(\alpha_i/S_i) \end{array}\right]}, \quad (26)$$

$$\frac{D_\alpha^{Fs}}{D_{\tan\varphi}^{Fs}} = \frac{D_\alpha^T - D_\alpha^S}{D_{\tan\varphi}^T - D_{\tan\varphi}^S} = \frac{\left[\begin{array}{l} \sum [c_i' b_i \sec\alpha_i \tan\alpha_i - \\ (W_i \sin\alpha_i + u_i b_i \sec\alpha_i \tan\alpha_i)\tan\varphi_i'] \\ \cdot\sum \frac{\alpha_i}{T_i} - \sum W_i \cos\alpha_i \cdot \sum \frac{\alpha_i}{S_i} \end{array}\right]}{\sum (W_i \cos\alpha_i - u_i b_i \sec\alpha_i)\cdot \sum \frac{\tan\varphi_i'}{T_i}}, \quad (27)$$

$$\frac{D_c^{Fs}}{D_u^{Fs}} = \frac{D_c^T - D_c^S}{D_u^T - D_u^S} = \frac{\sum b_i \sec\alpha_i \cdot \sum \frac{c_i'}{T_i}}{-\sum b_i \sec\alpha_i \tan\varphi_i' \cdot \sum \frac{u_i}{T_i}}. \quad (28)$$

The sensitivity ratio between different parameters is determined using eqs (25), (26) and (28). One can get a certain safety factor and come up with the sensitivity ratio between two different parameters using the specified procedures. Since there are four equations and five variables, the problem becomes statically indeterminate. However, superimposition of the sensitivity of the five parameters into one yields a statically determinate equation. A normalization technique can be used to determine the sensitivity of each parameter.

The relative sensitivity of the five parameters is given in eq. (29)

$$d_W^{Fs}|:|d_{\tan\varphi}^{Fs}|:|d_c^{Fs}|:|d_\alpha^{Fs}|:|d_u^{Fs}|$$
$$= |D_W^{Fs}|:|D_{\tan\varphi}^{Fs}|:|D_c^{Fs}|:|D_\alpha^{Fs}|:|D_u^{Fs}|. \quad (29)$$

Equation (30) meets

$$|d_W^{Fs}| + |d_{\tan\varphi}^{Fs}| + |d_c^{Fs}| + |d_\alpha^{Fs}| + |d_u^{Fs}| = 1. \quad (30)$$

Here d_x^{Fs} is the relative sensitivity of a safety factor, which shows the level of influence of each parameter at a certain slipping surface.

Case study

In this article, a commercially available two-dimensional limit equilibrium-based programme, the so-called Rocscience slide[15] was used for the analysis, using the Swedish arc method.

A typical case study with uniform slope was considered. The geometry of the slope has a height, $H = 30$ m, and a slope angle, $\beta = 30°$. The level of the groundwater table is shown in Figure 1.

The prevailing geotechnical parameters[16] are listed in Table 1.

The model was created and analysed using a comprehensive slope stability evaluation programme (slide). Three different slip surfaces were established by using three different radii. Typical results of the analysis are shown in Figure 2.

Table 1. Soil parameters

	γ (kN/m^3)	c (kPa)	φ (°)
Unsaturated unit weight	18.0	20.5	35
Saturated unit weight	20.0		

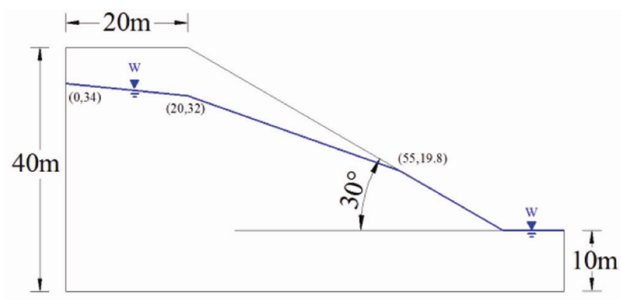

Figure 1. The geometry of a given slope.

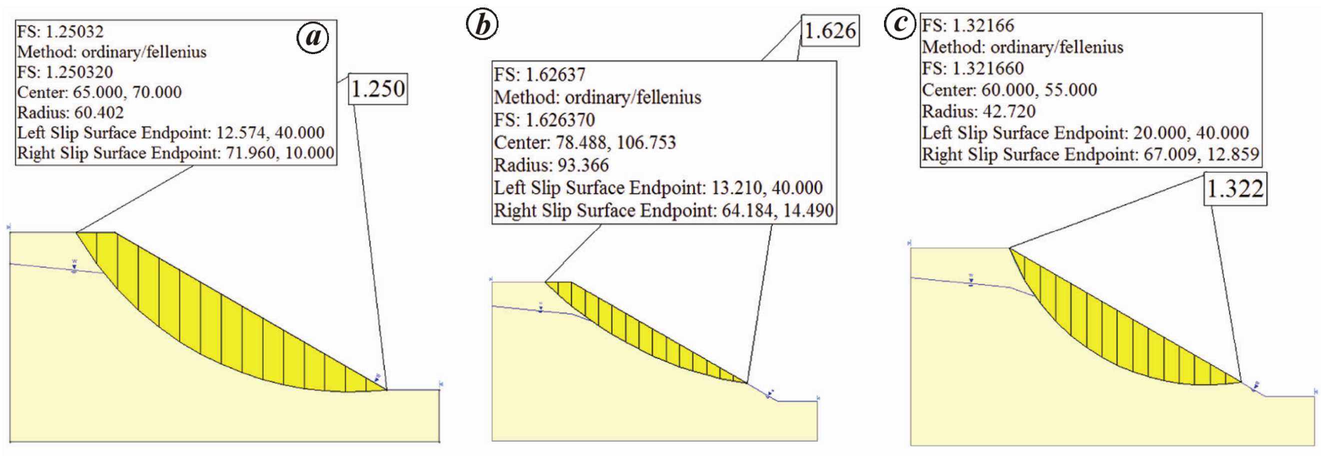

Figure 2. Results of different slip surfaces. ***a***, Slipping surface 1; ***b***, Slipping surface 2; ***c***, Slipping surface 3.

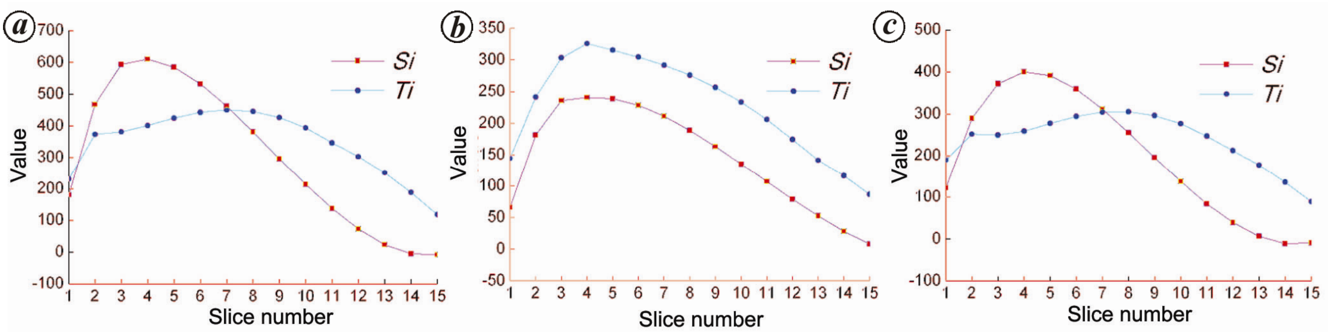

Figure 3. Skid resistance force and skid force distribution. ***a***, Slip surface 1; ***b***, Slip surface 2; ***c***, Slip surface 3.

Using the theoretical method

Based on the results of the software analysis, the statistical summaries for each slip surface are listed in Table 2.

After careful examination of Table 2 in the ascending order of the slices, the following conclusions were pointed out. The weight of slice and the pore water pressure increased up to a certain number of slices and then decreased. Angle of slip surface was decreased gradually, in line with the slip law of common slope. An attempt was made to study the relationship between the slide force, S_i and the skid resistance force, T_i as shown in Figure 3.

The slide force rapidly increased till it reached a certain value and then dramatically decreased (Figure 3). Unlike the slide force, the skid resistance force slightly increased till it reached a peak value and then decreased gradually. Meanwhile, the slide force attained its peak value earlier than the skid resistance force. Starting from slice No. 2 to slice No. 7, the slide force was higher than the skid resistance force (considering slipping surface 1). Then the slide force became steady and it was exceeded by the skid resistance force for the rest of slices. Therefore, improving the skid resistance force for slice No. 2 to slice No. 7 is an important task.

Regarding slip surface 2, the skid resistance force was higher than the slide force. Therefore, strengthening of the skid resistance force was not required in this case.

However, stabilization of the skid resistance force is an important issue for slice Nos 2 to 7 as shown in Figure 3*c*. For this particular case, piles are used to overcome the instability problem.

The effect of different parameters on the slope stability was computed and tabulated in Table 3.

Similarly, the sensitivity ratio between different parameters was determined and summarized in Table 4.

The minus sign shows the negative correlation between two parameters. As seen from Tables 3 and 4, since slip surface 1 develops negative slope angle close to cut export, the slide force and skid resistance force caused by gravity are conducive to the stability of the slope; so D_W^S is negative, D_W^T and D_W^{Fs} are positive; based on the comparison made on the three different slip surfaces, the stability of the slope was predominantly affected by the angle of the slip surface. The values of $d_{\tan\varphi}^{Fs}$ were almost steady in all cases. Hence, the shear strength parameter ($\tan\varphi$) played a noticeable role on the stability of the slope. The angle of a slip surface exhibited more influence on the cohesion and the weight of the soil than the internal angle of friction.

Table 2. Statistical summaries for different slip surfaces

	Sliding surface 1					Sliding surface 2					Sliding surface 3				
i	α (°)	W (kN)	u (kPa)	Si	Ti	α (°)	W (kN)	u (kPa)	Si	Ti	α (°)	W (kN)	u (kPa)	Si	Ti
1	56.79	215.49	0	180.29	230.82	42.94	96.7	0	65.87	144.73	64.55	134.68	0	121.61	190.02
2	50.41	607.24	5.79	467.97	373.13	40.15	281.06	0	181.21	241.57	55.9	349.82	0	289.67	251.92
3	44.82	841.8	38.65	593.33	381.5	37.47	388.14	0	236.12	303.48	48.95	493.16	22.37	371.9	249.88
4	39.73	953.96	60.54	609.69	401.08	34.88	421.38	0.36	240.99	325.91	42.88	588.2	43.57	400.23	259.04
5	34.99	1020.09	76.72	584.97	424.63	32.38	446.16	10.92	238.92	315.54	37.36	645.46	58.85	391.71	277.57
6	30.52	1048.37	88.21	532.37	442.74	29.94	457.82	19.47	228.49	304.73	32.23	673.46	69.56	359.19	294.4
7	26.24	1044.21	95.69	461.75	450.54	27.56	456.53	26.14	211.23	291.82	27.38	677.33	76.49	311.49	304.47
8	22.12	1011.38	99.61	380.88	445.58	25.23	443.15	31.06	188.9	275.99	22.73	660.42	80.17	255.21	305.43
9	18.12	952.56	100.31	296.24	426.73	22.95	418.39	34.35	163.11	256.68	18.24	625.02	80.95	195.64	296.27
10	14.21	869.7	98.03	213.43	393.73	20.7	382.84	36.07	135.32	233.48	13.86	572.7	79.08	137.21	276.76
11	10.36	763.91	92.95	137.37	346.74	18.48	337.01	36.32	106.85	206.14	9.57	504.57	74.75	83.85	247.21
12	6.56	631.43	78.23	72.14	302.64	16.3	281.31	35.13	78.95	174.54	5.32	419.8	65.71	38.94	212.38
13	2.79	476.1	58.99	23.17	250.52	14.14	214.79	31.04	52.46	141.53	1.11	317.5	49.69	6.14	177.47
14	–0.97	300.09	37.18	–5.08	188.19	12	135.3	19.53	28.12	116.38	–3.1	200.68	31.41	–10.85	135.63
15	–4.73	103.47	12.82	–8.54	117.98	9.87	46.58	6.72	7.99	86.61	–7.32	69.33	10.85	–8.84	88.92
Σ				4539.97	5176.55				2164.53	3419.13				2943.11	3567.35

Table 3. Effect of different parameters on the slope stability

Number of slip surface	D_W^S	D_α^S	D_W^T	D_α^T	$D_{\tan\varphi}^T$	D_u^T	D_c^T	D_W^{Fs}	D_α^{Fs}	$D_{\tan\varphi}^{Fs}$	D_c^{Fs}	D_u^{Fs}
1	–84.55	322.62	270.74	–58.93	186.84	72.28	–130.01	355.29	–381.55	186.84	72.28	–130.01
2	266.26	319.00	188.49	–36.29	171.57	91.28	–58.09	–77.77	–355.29	171.57	91.28	–58.09
3	364.85	318.45	245.77	–47.36	166.88	85.15	–124.49	–119.08	–365.81	166.88	85.15	–124.49

Table 4. Sensitivity ratio between different parameters

Number of slip surface	$D_{\tan\varphi}^{Fs}/D_c^{Fs}$	D_W^{Fs}/D_α^{Fs}	$D_\alpha^{Fs}/D_{\tan\varphi}^{Fs}$	$D_W^{FS}/D_{\tan\varphi}^{Fs}$	D_α^{Fs}/D_u^{Fs}	$d_{\tan\varphi}^{Fs}$	d_c^{Fs}	d_W^{Fs}	d_α^{Fs}	d_u^{Fs}
1	2.58	–0.93	–2.04	1.90	2.93	0.19	0.34	0.06	0.30	0.11
2	1.88	0.22	–2.07	–0.45	6.12	0.21	0.47	0.12	0.11	0.09
3	1.96	0.33	–2.19	–0.91	2.94	0.19	0.40	0.09	0.17	0.15

The relative sensitivity can be used to study the effect of different parameters on the stability of a given slope.

Conventional single-factor sensitivity analysis

In slope stability analysis, a safety factor is used as the main indicator to determine the stability of a particular slope. Therefore, it is regarded as system characteristics. First, a system has to be set up, and its system characteristics should be defined as $Fs = f(x_1, x_2, ..., x_n)$ (where x_i stands for different parameters). When the system characteristic meets $Fs^* = f(x^*)$, the corresponding design points will be $x^* = (x_1^*, x_2^*, ..., x_n^*)$. A parametric study can be done to study the level of influential parameters on the safety factor (Fs). In reality the units of each parameter are different.

Comparisons are made on it using dimensionless parameter s. Hence, the sensitivity of $D_{x_i}^{Fs}$ can be expressed as

$$D_{x_i}^{Fs} = \left| \frac{\Delta Fs/Fs}{\Delta x_i/x_i} \right|, \tag{31}$$

where $\Delta Fs/Fs$ is the relative change in safety factors Fs, and $|\Delta x_i/x_i|$ is the relative change in parameters, x_i. If the value of $D_{x_i}^{Fs}$ is high, the parameter, x_i will have considerable effect on Fs.

The sensitivity ratio between different parameters can be mathematically expressed as

$$\frac{D_{x_i}^{Fs}}{D_{x_j}^{Fs}} = \frac{\left| \dfrac{\Delta Fs/Fs}{\Delta x_i/x_i} \right|}{\left| \dfrac{\Delta Fs/Fs}{\Delta x_j/x_j} \right|} = \left| \frac{\dfrac{\partial Fs}{\partial x_i} \cdot \dfrac{x_i}{Fs}}{\dfrac{\partial Fs}{\partial x_j} \cdot \dfrac{x_j}{Fs}} \right|. \tag{32}$$

In the conventional method, the sensitivity of other parameters is considered to be constant. Moreover, the parameters are varied into a certain range to study the sensitivity of the parameters over the safety factor. In practice, many scholars ignore the sensitivity of parameters on the slope failure mode. In the meantime, sensitivity analysis often ignores the impact of new parameters introduced due to the new failure mode. The sensitivity analyses employed will be discussed in detail.

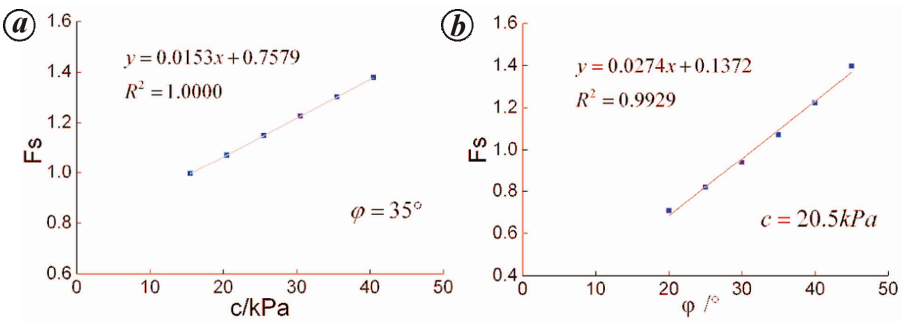

Figure 4. Relationships between the safety factor and the shear strength parameters. ***a***, Cohesion; ***b***, Friction angle.

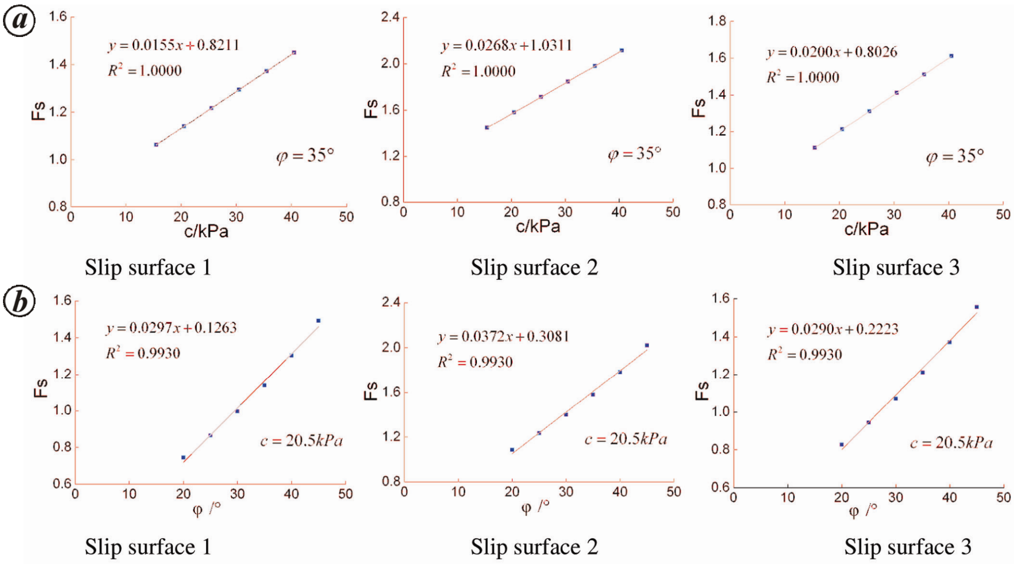

Figure 5. Relationships between the safety factor and the shear strength parameters. ***a***, Relationships between the safety factor and the cohesion (when the value of the internal angle of friction was constant). ***b***, Relationships between the safety factor and the internal angle of friction (when the value of cohesion was constant).

Automatic search slip surface: To verify the accuracy of results, the sensitivity of the shear strength parameters on the safety factor was done using an automatic search slip surface technique. During the computation of safety factors, one parameter was allowed to vary while the other parameter was kept constant. Figure 4 shows the trend of safety factors for the corresponding shear strength parameters.

One can understand that the safety factor exhibited a relatively strong linear correlation with the cohesion than the internal angle of friction.

Fixed slip surface: The safety factors (for a fixed slip surface case) were similarly computed by varying one parameter while the other was constant. Here again, Figure 5 shows the trend of safety factors for the corresponding shear strength parameters.

According to the lessons learnt from Figures 4 and 5, one should not ignore the effect of slide force on the sensitivity analysis.

Comparative study on different methods: In the above Figures 4 and 5, the sensitivity ratio, $(D^{Fs}_{\tan\varphi} / D^{Fs}_{c})$ was determined using eq. (32). The results are summarized in Table 5.

After careful study of Table 5, the following conclusions were pointed out.

(1) In the case of fixed slip surface, the results obtained from the theoretical analysis showed good agreement with the conventional one. However, the conventional single-factor sensitivity analysis yielded higher value of results than the theoretical ones. This phenomenon occurred due to the assumption made on conventional single-factor sensitivity analysis. In fact, there is a strong interaction among different parameters. Hence, the theoretical analysis is reasonable.

(2) Coming to the conventional method, the effect of parameter variations on the failure path is often ignored during sensitivity analysis. A particular complex slope mass will have a multiple structural surface with a new parameter affecting its stability. Therefore, its effect on the results of sensitivity analysis cannot be eliminated.

(3) For a given failure surface, unstable slope will have a high value of sensitivity ratio in the shear strength parameters $(D^{Fs}_{\tan\varphi}/D^{Fs}_{c})$.

Table 5. Results of the comparative study on the different methods

Slip surfaces	Theoretical derivation method/ ($D_{\tan\varphi}^{Fs}/D_c^{Fs}$)	Single-factor sensitivity analysis ($D_{\tan\varphi}^{Fs}/D_c^{Fs}$)		Safety factor/Fs
		Automatic search slip surface	Fixed slip surface	
1	2.58	2.863	2.849	1.250
2	1.88		1.937	1.626
3	1.96		2.039	1.322

(4) The theoretical analysis approach is used to determine the sensitivity ratio of different parameters at any slipping surface. Therefore, the role of different parameters on the slope stability can be studied to provide efficient slope protection measures.

Conclusion

The following conclusions are made from our studies.

(1) The theoretical analysis approach is an accurate tool. (2) Based on the findings of this paper, the sensitivity analysis method has the following four advantages: (a) The sensitivity ratio can be conducted between two parameters in a theoretical manner. Besides, it can also be used to overcome the drawbacks of the conventional approach. (b) It can be used to determine the safety factor and the sensitivity ratio between different parameters. Moreover, the role of different parameters on the stability of slopes can be studied by this method and an efficient and economical slope protection measure can be provided. (c) The method used has a well-developed theoretical background, and it does not consider the correlation between parameters. In the meantime, the discrepancy between the parameters can be eliminated using effective stress analysis. (d) It can carry out a sensitivity analysis on the angle of a slip surface, α. The conventional method requires creation and calculation of multiple models. Moreover, it has some computational difficulties due to the variations in the angle of the slip surface. Unfortunately, the numerical model cannot address this problem. (3) The theoretical derivations can be applied into different slope stability analysis, such as: Bishop slice method, Yang cloth slice method, etc. Effective stress analysis can even be used to determine the sensitivity analysis of complex structures.

Further studies are recommended to develop a computer program based on theoretical derivations made in this study. The authors believe that the present findings will have an indispensible role to understand and capture the nature of geotechnical problems.

1. Zhang, W.-G. and Liu, Y., Main factor sensitivity analysis based on response surface model updating of port crane structure. *J. Coastal Res*., 2015, **73**, 166–172.
2. Singh, N. and McFarland, E. W., Leveled cost of energy and sensitivity analysis for the hydrogen-bromine flow battery. *J. Power Sources*, 2015, **288**, 187–198.
3. De Staelen, R. H. and Beddek, K., Sensitivity analysis and variance reduction in a stochastic non-destructive testing problem. *Int. J. Comput. Math*., 2015, **92**(9), 1874–1882.
4. Ma, C. F., Li, X. and Wang, S. G., A global sensitivity analysis of soil parameters associated with back scattering using the advanced integral equation model. *IEEE T. Geosci. Remote*, 2015, **53**(10), 5613–5623.
5. Schattler, H. and Ledzewicz, U., Fields of extremals and sensitivity analysis for multi-input bilinear optimal control problems. *Discrete Cont. DYN-A*, 2015, **35**(9), 4611–4638.
6. Boyaghchi, F. A. and Molaie, H., Sensitivity analysis of exergy destruction in a real combined cycle power plant based on advanced exergy method. *Energ. Convers. Manage*., 2015, **99**, 374–386.
7. Bodjona, K. and Lessard, L., Load sharing in single-lap bonded/bolted composite joints. Part II: global sensitivity analysis. *Compos. Struct*., 2015, **129**, 276–283.
8. Bonstrom, H. and Corotis, R. B., Optimizing portfolio loss reduction using a first-order reliability method sensitivity analysis. *Struct. Infrastruct. E*, 2015, **11**(9), 1190–1198.
9. Park, W., Park, J. and Kim, H. K., Candidate model construction of a cable-stayed bridge using parameterized sensitivity-based finite element model updating. *Struct. Infrastruct. E*, 2015, **11**(9), 1163–1177.
10. Pianosi, F., Sarrazin, F. and Wagener, T., A MATLAB toolbox for global sensitivity analysis. *Environ. Modell. Softw.,* 2015, **70**, 80–85.
11. Chastaing, G. and LeGratiet, L., ANOVA Decomposition of conditional Gaussian processes for sensitivity analysis with dependent oinputs. *J. Stat. Comput. Sim*., 2015, **85**(11), 2164–2186.
12. Li, D. Q., Jiang, S. H., Cao, Z. J., Zhou, W., Zhou, C. B. and Zhang, L. M., A multiple response-surface method for slope reliability analysis considering spatial variability of soil properties. *Eng. Geol*., 2015, **187**, 60–72.
13. Wan, L. P., Liu, J., Zhao, Z. Y., Dong, Y. H. and Cheng, Z., Layered sensitivity analysis and weight determination of rock slope stability impacting factors. *Water Resour. Hydr. Eng*., 2015, **43**(3), 59–62.
14. He, B. G., Gao, Q. and Liu, F., Orthogonal analysis and numerical simulation on influential factors of freeway slope stability. *Chinese J. Geotech. Eng.*, 2015, **27**(6), 716–719.
15. Toronto Rocscience Inc., *Rocscience Slide*, Version 6.0 (Toronto).
16. Toronto Rocscience Inc.. *Slide Verification Manual[R]*, Rocscience Inc., Toronto, 2003.

ACKNOWLEDGEMENT. This research was supported by the national natural science fund projects 51439003 and 51679127.

Received 6 September 2016; revised accepted 23 May 2017

doi: 10.18520/cs/v113/i11/2097-2104